openheart

Detection of cardiac amyloidosis using machine learning on routine echocardiographic measurements

Rachel Si-Wen Chang ,[1] I-min Chiu,[2] Phillip Tacon,[2] Michael Abiragi,[2] Louie Cao,[2] Gloria Hong,[2] Jonathan Le,[2] James Zou,[3] Chathuri Daluwatte,[4] Piero Ricchiuto,[4] David Ouyang[2]

► Additional supplemental material is published online only. To view, please visit the journal online (https://doi.org/10.1136/openhrt-2024-002884).

To cite: Chang RS-W, Chiu I, Tacon P, *et al*. Detection of cardiac amyloidosis using machine learning on routine echocardiographic measurements. *Open Heart* 2024;**11**:e002884. doi:10.1136/openhrt-2024-002884

Received 18 August 2024
Accepted 12 November 2024

[1]UCSF, San Francisco, California, USA
[2]Cedars-Sinai Medical Center, Los Angeles, California, USA
[3]Stanford University, Stanford, California, USA
[4]Alexion Pharmaceuticals, Boston, Massachusetts, USA

Correspondence to
Dr David Ouyang; david.ouyang@cshs.org

ABSTRACT

Background Cardiac amyloidosis (CA) is an underdiagnosed, progressive and lethal disease. Machine learning applied to common measurements derived from routine echocardiogram studies can inform suspicion of CA.

Objectives Our objectives were to test a random forest (RF) model in detecting CA.

Methods We used 3603 echocardiogram studies from 636 patients at Cedars-Sinai Medical Center to train an RF model to predict CA from echocardiographic parameters. 231 patients with CA were compared with 405 control patients with negative pyrophosphate scans or clinical diagnosis of hypertrophic cardiomyopathy. 19 common echocardiographic measurements from echocardiogram reports were used as input into the RF model. Data was split by patient into a training data set of 2882 studies from 486 patients and a test data set of 721 studies from 150 patients. The performance of the model was evaluated by area under the receiver operative curve (AUC), sensitivity, specificity and positive predictive value (PPV) on the test data set.

Results The RF model identified CA with an AUC of 0.84, sensitivity of 0.82, specificity of 0.73 and PPV of 0.76. Some echocardiographic measurements had high missingness, suggesting gaps in measurement in routine clinical practice. Features that were large contributors to the model included mitral A-wave velocity, global longitudinal strain (GLS), left ventricle posterior wall diameter end diastolic (LVPWd) and left atrial area.

Conclusion Machine learning on echocardiographic parameters can detect patients with CA with accuracy. Our model identified several features that were major contributors towards identifying CA including GLS, mitral A peak velocity and LVPWd. Further study is needed to evaluate its external validity and application in clinical settings.

WHAT IS ALREADY KNOWN ON THIS TOPIC

⇒ Cardiac amyloidosis (CA) is an underdiagnosed, progressive and lethal disease and it is difficult to diagnose it. Artificial intelligence is increasingly being used to help detect diseases. Echocardiography, a commonly used cardiac imaging study, has been used in deep-learning models to assist in the identification of CA.

WHAT THIS STUDY ADDS

⇒ Our study demonstrates that common echocardiographic measurements can be used in machine-learning models to detect CA with accuracy. Our random forest model identified CA with an area under the receiver operative curve of 0.84, sensitivity of 0.82, specificity of 0.73 and positive predictive value of 0.76. The accuracy of our model was comparable in performance with previously published approaches using other input data including ECG waveforms, echocardiogram images and electronic health records.

HOW THIS STUDY MIGHT AFFECT RESEARCH, PRACTICE OR POLICY

⇒ Our study has shown that in patients who are suspected of having CA, machine learning models that use common echocardiographic measurements can be used to detect CA with accuracy. Future studies should prospectively evaluate the performance of machine learning models using echocardiographic features to detect CA and other diseases. Future applications of our model to detect CA include use in screening echocardiogram databases or implementation as part of the workflow in evaluating patients who are deemed at high clinical risk of CA.

INTRODUCTION

Cardiac amyloidosis (CA) is a progressive and lethal disease resulting from the deposition of amyloid protein into myocardial tissue. Amyloid deposits consist of misfolded proteins that form fibrils and accumulate in tissue.[1] This amyloid deposition in the heart can result in restrictive cardiomyopathy, leading to heart failure, arrhythmias and ultimately death. CA is often diagnosed late; once diagnosed, untreated patients live only an average of a few years from the time of diagnosis.[2 3] With the development of multiple new therapeutics, early identification and treatment of CA is of increasing importance.

CA is likely underdiagnosed in common clinical practice, likely due to the non-specific symptoms patient experience that span across all types of heart failure. In cohorts undergoing focused evaluation for CA, the prevalence of CA seems higher. CA can be seen in around 13–17% of patients with heart failure with preserved ejection fraction.[4 5] Additionally, CA is seen in up to 16% of patients with degenerative aortic stenosis.[6] In autopsy studies, transthyretin amyloid (ATTR) deposits have been found to be present in the heart of up to 25% of patients aged 80 or older.[7] New disease-modifying drugs have been shown to improve survival and reduce hospitalisations in patients with CA;[8] however, data suggests more benefit when administered earlier in the course of the disease,[9] underscoring the importance of timely diagnosis.

Echocardiography, the most common form of cardiac imaging, is often obtained in patients with heart failure symptoms and contains multiple findings that can be suggestive of CA.[10] While echocardiography is common, cost-effective and accessible, it is limited in the diagnosis of CA by subjective human interpretation[11] and variability in interpretation.[12] Studies have demonstrated deep learning models applied to medical imaging can derive precise measurements and identify characteristics informative of future risk.[13 14] Echocardiography in particular has been used in studies examining deep learning algorithms to automate the screening and identification of CA.[15 16]

While more complicated artificial intelligence (AI) models have been developed to assess ECG waveforms and echocardiogram videos, there has been limited work on repurposing commonly acquired conventional measurements to help inform suspicion of CA. Such approaches, including previously evaluated approaches using electronic health record elements[17] such as diagnosis codes, have shown promising results with lower barriers to entry for adoption. In particular, we were interested in conventional machine learning methods such as random forest (RF) models which are well suited for dealing with the non-linear and complex relationships that are often present in medical data. In our study, we investigated whether machine learning on routine echocardiographic measurements can assist in the detection of CA (figure 1).

METHODS

Study setting

We conducted a retrospective analysis of patients with CA who had echocardiography studies obtained at Cedars-Sinai Medical Center between 1 January 2007 and 31 August 2023. The patients with CA were compared against a combination of patients who had high clinical and echocardiographic suspicion for CA but were ruled out. These control patients included patients who received negative cardiac pyrophosphate (PYP) scans as well as patients eventually diagnosed with hypertrophic CA. We used this population in order to best train our model to detect CA with accuracy. A total of 636 patients were included in the analysis and all transthoracic echocardiogram studies were used. Data was split at the patient level in a 4:1 ratio between training and validation data sets. For patients with multiple echocardiogram studies, each study was treated as an independent data point in our analysis within the same split.

Clinical data for patients was extracted from electronic medical records including demographics and medical comorbidities. We chose common cardiometabolic comorbidities to help characterise our patient population such as hypertension, diabetes mellitus, coronary artery disease and atrial fibrillation. All forms of CA were included in the cases including both TTR and immunoglobulin light chain (AL) CA and were identified through both our advanced heart failure registry and a list of patients with a positive PYP scan. Medical comorbidities were determined through the International Classification of Diseases 9th and 10th edition codes.

Machine learning

We developed a RF model due to its several intrinsic advantages for our task. The most common echocardiogram measurements (present in at least 65% of cases) were used to build the machine learning model. We used only standardly measured echocardiogram measurements to build our model, as many CA hallmarks such as pericardial effusion or strain relative apical sparing are not routinely measured. We inputted missing values for each feature with median values from the existing values. Global longitudinal strain (GLS) measurements, not commonly reported in clinical echocardiogram studies, were manually and prospectively measured using TomTec imaging software; this was measured blind to patient characteristics. Echocardiograms in which the patient was in atrial fibrillation were excluded. Ultimately, 19 common echocardiographic measurements from echocardiogram reports were used for the model (online supplemental table 1). All features' values were scaled using minimal–maximal normalisation into 0–1.

During training, we set the hyperparameter of RF using a number of trees as 100, minimal samples split as 2 and minimal samples leaf as 1, employing the Gini impurity criterion to measure node purity in the data set. We implemented a stepwise feature selection protocol using the RF model to identify the most informative subset of features for predicting CA. This process began with an empty feature set and iteratively added features that maximised the area under the receiver operating curve (AUC) value. In each round, the feature that provided the highest increase in AUC was retained and the model was retrained to assess the cumulative effect on performance. This iterative approach continued until the addition of new features failed to improve the AUC for three consecutive rounds. This feature selection strategy not only identified the most predictive subset of features but also helped mitigate overfitting by limiting the model complexity. The result was a robust set of features that

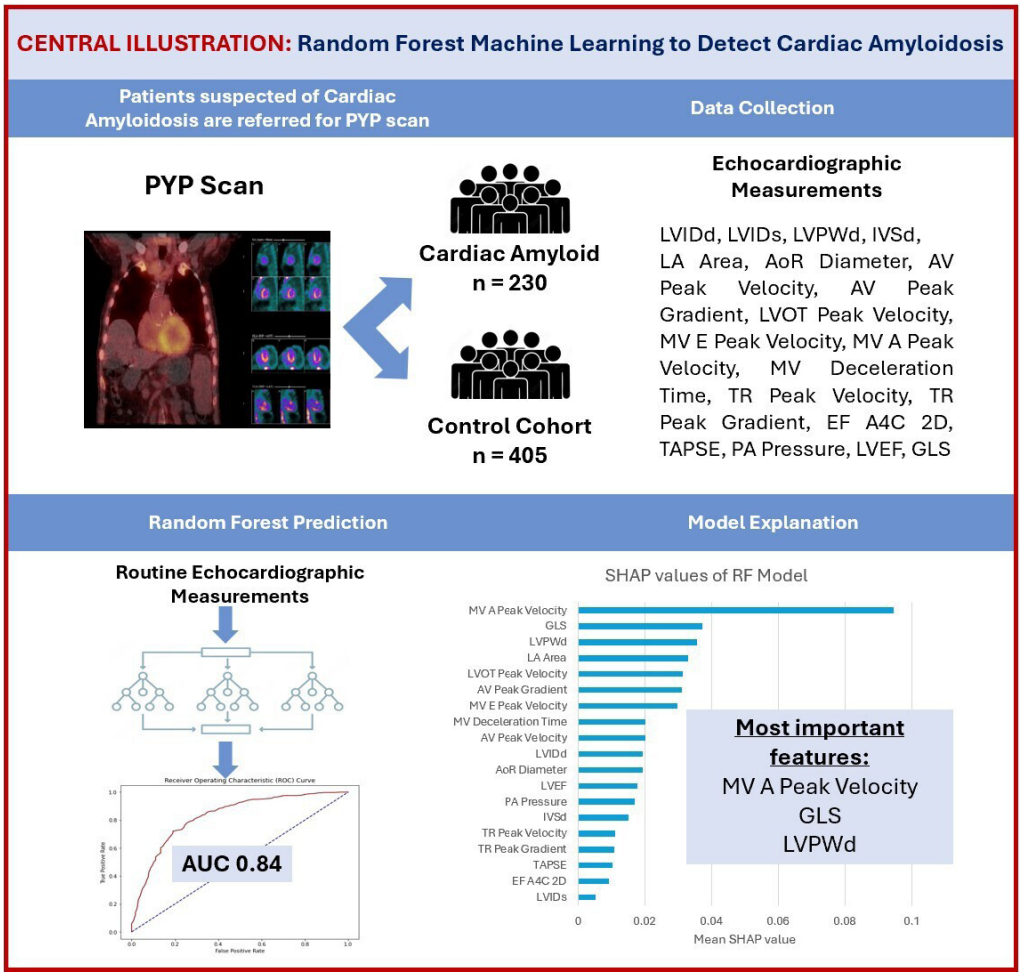

Figure 1 Development and evaluation of a random forest model to predict cardiac amyloidosis. AoR, aortic root; AUC, area under the receiver operative curve; AV, aortic valve; EF, ejection fraction; GLS, global longitudinal strain; IVSd, interventricular septal end diastole; LA, left atrium; LVEF, left ventricular ejection fraction; LVIDd, left ventricular internal diameter end diastole; LVIDs, left ventricular internal diameter end systole; LVOT, left ventricular outflow track; LVPWd, left ventricular posterior wall end diastole; MV, mitral valve; PA, pulmonary artery; PYP, pyrophosphate; RF, random forest; SHAP, SHapley Additive exPlanations; TAPSE, tricuspid annular plane systolic excursion; TR, tricuspid regurgitation.

contributed to the model's predictive capabilities with the best feature achieving the highest individual AUC. Models trained with fewer features did not yield as high AUC.

Statistical analysis

In this study, we used non-parametric methods for statistical inference. Continuous variables were summarised as median (IQR) or mean (SD) if normally distributed whereas categorical variables were summarised using counts and percentages. Mean values of each echocardiogram feature were calculated and p values were generated. The performance of the model was evaluated by AUC, sensitivity, specificity and positive predictive value (PPV). A SHapley Additive exPlanations (SHAP) algorithm was used to interpret the RF model to show the impact of each feature on the model in order of importance. SHAP values were used to determine the significance of each feature in the model. The development of the machine learning model and statistical analysis was conducted using Python V.3.8.13 with scikit-learn V.0.24.2 and SciPy Package V.1.10.1.

RESULTS

Our data set consisted of 3603 echocardiograms from 636 patients at Cedars-Sinai Medical Center between 1 January 2007 and 31 August 2023. The median age was 72 (62–81) years. 69.2% were men, 61.9% had hypertension, 40.9% had diabetes mellitus, 40.9% had coronary artery disease and 38.5% had atrial fibrillation (table 1). 231 patients were diagnosed with CA and had 1581 echocardiograms in the study period. Of these patients, 55 (23.8%) had AL, 91 (39.4%) had ATTR and 85 (36.8%) had an unspecified subtype of CA. The control group consisted of 405 patients with 2022 echocardiograms. The cohort was split into 486 patients (2882 studies) for training and 150 patients (721 studies) for testing (figure 2).

The RF model used 19 features from echocardiogram reports. Mean values of these features in cases and

Table 1 Baseline participant characteristics

	All (N=636)	Amyloid (N=231)	Non-amyloid (N=405)
	Median (IQR) or N (%)	Median (IQR) or N (%)	Median (IQR) or N (%)
Age	72 (62–81)	72 (63–79)	72 (62–81)
Men	440 (69.2)	188 (81.4)	247 (61.0)
Subtype			
AL		55 (23.8)	
ATTR		91 (39.4)	
Unspecified		85 (36.8)	
Hypertension	394 (61.9)	134 (58.0)	260 (64.2)
Diabetes mellitus	260 (40.9)	81 (35.1)	179 (44.2)
Coronary artery disease	260 (40.9)	93 (40.3)	167 (41.2)
Atrial fibrillation	245 (38.5)	110 (47.6)	135 (33.3)

AL, immunoglobulin light chain amyloidosis; ATTR, transthyretin amyloidosis.

controls are presented in table 2. Overall, patients with CA had lower mitral early-diastolic (E) peak velocities (82.87 (21.81) cm/s vs 98.11 (41.58) cm/s; p value<0.001), lower mitral end-diastolic (A) peak velocities (45.53 (17.14) cm/s vs 77.91 (38.89) cm/s; p value<0.001) and higher pulmonary artery pressures (34.96 (12.62) mm Hg vs 30.08 (13.35) mmHg; p value 0.002). Structurally, patients with CA had smaller left atrial (LA) areas (24.19 (6.11) cm^2 vs 25.86 (10.15) cm^2; p value<0.001) and smaller chamber dimensions (left ventricular internal diameter end diastole 4.24 (1.23) vs 4.51 (0.82); p value<0.001). Functionally, patients with CA had lower left ventricular ejection fraction (LVEF) (56.63 (13.30)% vs 58.30 (14.50)%; p value<0.001) and lower tricuspid annular plane systolic excursion (TAPSE) (1.50 (0.74) mm vs 1.85 (0.98) mm; p value<0.001) compared with echocardiograms without CA.

Using all 19 echocardiogram features, our RF model identified CA with an AUC of 0.84. Sensitivity was 0.82 while specificity was 0.73; PPV was 0.76. When using a stepwise feature selection strategy, a parsimonious RF model using only 14 features had an AUC of 0.83, sensitivity of 0.79, specificity of 0.73 and PPV of 0.75 (table 3). The differential impact of each echocardiogram feature on the RF model was evaluated using the SHAP value (figure 3). Mitral A-wave velocity (MV A peak velocity) had the largest impact on model output. GLS, left ventricle posterior wall diameter end-diastolic (LVPWd), LA area, left ventricular outflow tract peak velocity, aortic valve peak gradient and mitral E-wave velocity also had large impacts on model output. Some echocardiogram features were not present in all echocardiograms, thus the frequency at which they were missing was determined (ie, a missingness rate) (online supplemental figure 1). GLS had the highest rate at 71.5%. TAPSE and MV A peak velocity were second highest at a missingness rate of 32.9%. The LA area had a missingness rate of 28.5%.

DISCUSSION

CA is an under-recognised disease but likely a more prevalent disease than previously recognised. In this study,

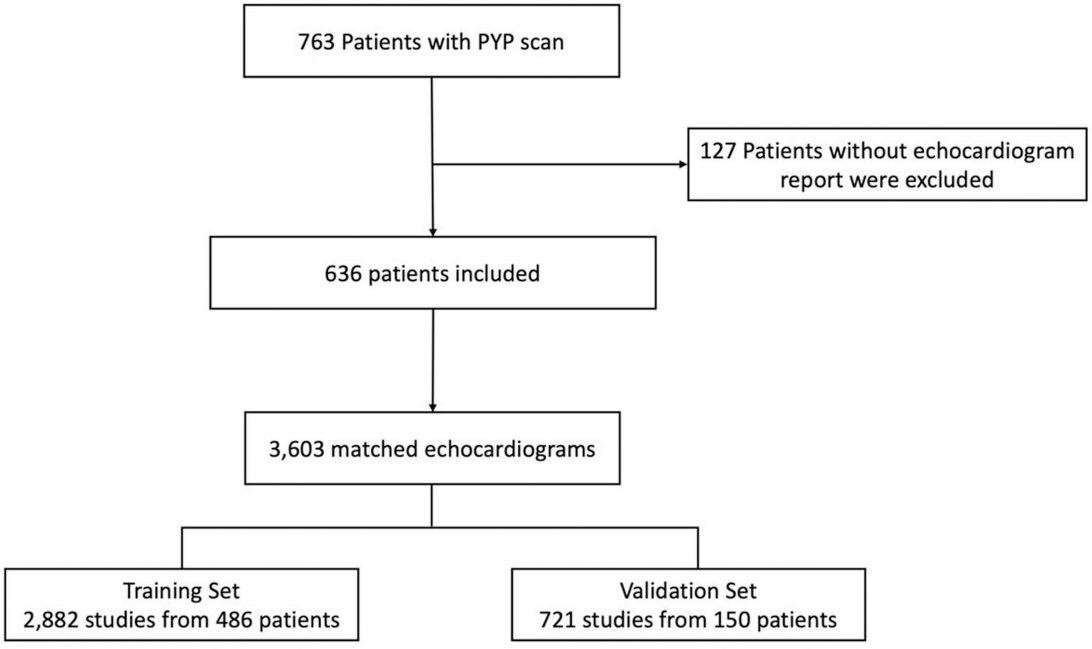

Figure 2 Workflow of selecting cases for RF model. Patients with PYP scans were identified and those without echocardiogram reports were excluded. The patients remaining were matched to their echocardiograms and a training set and validation set were created. PYP, pyrophosphate; RF, random forest.

Table 2 Mean echocardiogram features in echocardiograms with amyloid and echocardiograms without amyloid

	Without amyloid (N=2022)	With amyloid (N=1581)	
	Mean (SD)	Mean (SD)	P value
LVIDd (cm)	4.51 (0.82)	4.24 (1.23)	<0.001
LVIDs (cm)	3.09 (0.90)	2.96 (0.92)	<0.001
LVPWd (cm)	1.22 (0.27)	1.32 (0.39)	<0.001
IVSd (cm)	1.35 (0.42)	1.39 (0.42)	0.006
AoR diameter (cm)	3.23 (0.46)	3.21 (0.43)	0.421
AV peak velocity (cm/s)	179.08 (82.61)	127.00 (46.96)	<0.001
AV peak gradient (mm Hg)	15.77 (16.01)	7.41 (6.31)	<0.001
LVOT peak velocity (cm/s)	111.54 (64.55)	85.52 (22.66)	<0.001
MV deceleration time (cm/s)	229.23 (101.08)	180.24 (58.86)	<0.001
MV E peak velocity (cm/s)	98.11 (41.58)	82.87 (21.81)	<0.001
MV A peak velocity (cm/s)	77.91 (38.89)	45.53 (17.14)	<0.001
LA area (cm^2)	25.86 (10.15)	24.19 (6.11)	<0.001
TR peak velocity (cm/s)	256.23 (68.56)	251.92 (55.83)	0.077
TR peak gradient (mm Hg)	30.08 (13.25)	28.57 (12.32)	0.002
PA pressure (mm Hg)	30.08 (13.35)	34.96 (12.62)	0.002
TAPSE (cm)	1.85 (0.98)	1.50 (0.74)	<0.001
GLS (%)	−13.84 (5.16)	−9.59 (3.81)	<0.001
LVEF (%)	58.30 (14.50)	56.63 (13.30)	<0.001
EF A4C 2D (%)	58.34 (14.66)	56.32 (13.50)	<0.001

AoR, aortic root; AV, aortic valve; EF, ejection fraction; GLS, global longitudinal strain; IVSd, interventricular septal end diastole; LA, left atrium; LVEF, left ventricular ejection fraction; LVIDd, left ventricular internal diameter end diastole; LVIDs, left ventricular internal diameter end systole; LVOT, left ventricular outflow track; LVPWd, left ventricular posterior wall end diastole; MV, mitral valve; PA, pulmonary artery; TAPSE, tricuspid annular plane systolic excursion; TR, tricuspid regurgitation.

we demonstrated that machine learning (RF models) using echocardiogram features can distinguish between patients with CA versus non-CA with accuracy. By using common echocardiographic measurements, such an approach can be readily adapted from existing clinical databases to augment clinician suspicion of CA. We found our CA echocardiograms had diminished mitral velocities, consistent with restrictive physiology,[18] along with decreased systolic function. The accuracy of our model was comparable in performance to previously published approaches using other input data including ECG waveforms, echocardiogram images and EHR, potentially allowing for multimodal complementary approaches that augment the accuracy of any individual model.

In our model, we found several features that were prominent contributors towards predicting CA but had high missingness rates within echocardiogram reports. Both LVPWd and MV A peak velocity were important predictors of our model, though also had a high missingness rate (10.1% and 32.9%, respectively). Additionally, decreased GLS is often an early, sensitive sign of CA and a predictor of mortality in CA[19] and its predictive value was confirmed in our study. We found that GLS was the second most important echocardiogram feature that contributed to our model, though had a missing rate of 71.5% in our study. This may be due to GLS not being routinely measured on echocardiograms in the clinical setting, potentially due to variability between ultrasound machines and cost. However, GLS has increasingly been seen as an effective tool in prognosticating heart failure and may be superior to LVEF.[17 20] Increasing LVPWd, MV A peak velocity and GLS measurement in clinical settings, potentially through automation through AI, may improve early detection of CA.

With advances in treatment, it is crucial for the medical community to improve CA diagnosis. A consensus document from several organisations on multimodal imaging in CA recently made a call to action to further investigate machine learning-based modalities over standard approaches.[21] Recognition of CA is exceptionally important given the possibility of effective early treatment and recent literature has emphasised the education of providers in the detection of this disease.[22] In addition to tafamadis,[9] there are several emerging therapeutics under clinical trial investigation for the treatment of amyloidosis including TTR expression silencers, small-interfering ribonuclear acid agents and TTR stabiliser drugs.[23]

Future steps include external validation of the algorithm and its application in clinical settings, possibly through screening echocardiogram databases or implemented as part of the workflow in evaluating patients who are deemed at high clinical risk of CA.

Table 3 Random forest model performance metrics

	AUC	Sensitivity	Specificity	PPV
All 19 features	0.84	0.82	0.73	0.76
Feature selection (14 features)	0.83	0.79	0.73	0.75

AUC, area under the receiver operative curve; PPV, positive predictive value.

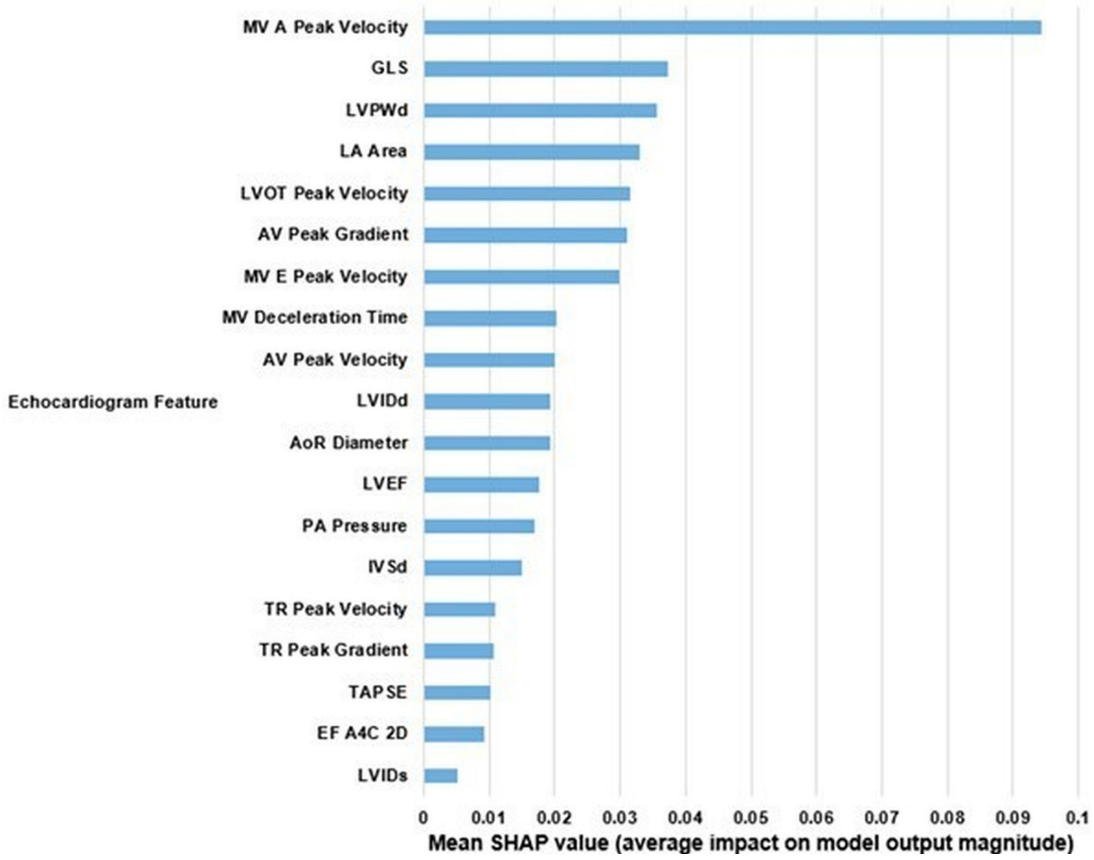

Figure 3 SHAP values of RF model. This model demonstrates the differential impact of each echocardiogram feature (y-axis) to the RF model measured through SHAP value (x-axis). AoR, aortic root; AV, aortic valve; EF, ejection fraction; GLS, global longitudinal strain; IVSd, interventricular septal end diastole; LA, left atrium; LVEF, left ventricular ejection fraction; LVIDd, left ventricular internal diameter end diastole; LVIDs, left ventricular internal diameter end systole; LVOT, left ventricular outflow track; LVPWd, left ventricular posterior wall end diastole; MV, mitral valve; PA, pulmonary artery; RF, random forest; SHAP, SHapley Additive exPlanations; TAPSE, tricuspid annular plane systolic excursion; TR, tricuspid regurgitation.

Limitations

A few limitations should be noted. Our study only includes echocardiogram data from Cedars-Sinai Medical Center, mainly deriving from patients in Los Angeles County; future work is needed to validate such an approach in external populations. While echocardiograms are not used for definitive diagnosis of CA, we focused on echocardiography as it is the most common form of cardiac imaging, making it a suitable candidate screening tool at the beginning of any diagnostic pathway. Even with high suspicion, further confirmatory tests such as the PYP scan are necessary for the definitive diagnosis of CA. Other limitations include the higher missingness values for some parameters including GLS. Additionally, our study groups together all types of CA, though they may have different echocardiographic features. Finally, the echocardiographic measurements used were only derived from common echocardiogram measurements; we did not include descriptive features such as the existence of pericardial effusion, severity of diastolic dysfunction or less common measurements such as right ventricular thickness.

CONCLUSION

CA is an under-recognised and progressive disease; advancements in machine learning can allow for improved detection of CA. Our study demonstrates the effectiveness of machine learning (RF models) in detecting CA through echocardiographic measurements in electronic health records. Furthermore, our model identified several features that were major contributors towards identifying CA including GLS, MV A peak velocity and LVPWd and some of these measurements have high missingness in EHR data suggesting gaps in measurement in routine clinical practice. Thus, increasing the measurement of these features in the clinical setting may aid in the detection of CA. While the model shows promise, external validation and further study are essential to determine its broader applicability in clinical settings.

X Rachel Si-Wen Chang @rachechang and Louie Cao @LouieCaoMD

Acknowledgements The authors would like to thank John Sekab, Julia Catini and Nan Zhang for their review and input to the manuscript.

Contributors RC, IC and DO contributed to conception of the project, data analysis and interpretation and drafting of the manuscript. CD and PR funded the study and

helped draft the final manuscript. IC assisted with model analysis. PT, MA, GH, LC, JL and JZ assisted in data collection and analysis and creation of machine learning model. DO is guarantor.

Funding This research was funded by Alexion.

Competing interests This research was funded by Alexion. CD and PR are employees of Alexion, AstraZeneca Rare Disease at the time of publication and may hold shares and/or stock options in the company. DO reports consulting fees from Ultromics, InVision, Echo IQ, Pfizer and research grants from NIH NHLBI and Alexion. All other authors report no disclosures to report.

Patient consent for publication Not applicable.

Ethics approval The Institutional Review Board of Cedars-Sinai Medical Center approved the study protocol. Participants gave informed consent to participate in the study before taking part.

Provenance and peer review Not commissioned; externally peer reviewed.

Data availability statement Data are available upon reasonable request. Raw data were generated at Cedar Sinai Medical Center. Derived data supporting the findings of this study are available from the corresponding author (DO) on request.

ORCID iD

Rachel Si-Wen Chang http://orcid.org/0000-0002-8969-2757

REFERENCES

1 Gillmore JD, Hawkins PN. Pathophysiology and treatment of systemic amyloidosis. *Nat Rev Nephrol* 2013;9:574–86.
2 Lane T, Fontana M, Martinez-Naharro A, *et al*. Natural History, Quality of Life, and Outcome in Cardiac Transthyretin Amyloidosis. *Circulation* 2019;140:16–26.
3 Grogan M, Scott CG, Kyle RA, *et al*. Natural History of Wild-Type Transthyretin Cardiac Amyloidosis and Risk Stratification Using a Novel Staging System. *J Am Coll Cardiol* 2016;68:1014–20.
4 González-López E, Gallego-Delgado M, Guzzo-Merello G, *et al*. Wild-type transthyretin amyloidosis as a cause of heart failure with preserved ejection fraction. *Eur Heart J* 2015;36:2585–94.
5 Mohammed SF, Mirzoyev SA, Edwards WD, *et al*. Left ventricular amyloid deposition in patients with heart failure and preserved ejection fraction. *JACC Heart Fail* 2014;2:113–22.
6 Castano A, Haq M, Narotsky DL, *et al*. Multicenter Study of Planar Technetium 99m Pyrophosphate Cardiac Imaging: Predicting Survival for Patients With ATTR Cardiac Amyloidosis. *JAMA Cardiol* 2016;1:880–9.
7 Cornwell GG, Murdoch WL, Kyle RA, *et al*. Frequency and distribution of senile cardiovascular amyloid. A clinicopathologic correlation. *Am J Med* 1983;75:618–23.
8 Benson MD, Waddington-Cruz M, Berk JL, *et al*. Inotersen Treatment for Patients with Hereditary Transthyretin Amyloidosis. *N Engl J Med* 2018;379:22–31.
9 Stern LK, Patel J. Cardiac Amyloidosis Treatment. *Methodist Debakey Cardiovasc J* 2022;18:59–72.
10 Kittleson MM, Maurer MS, Ambardekar AV, *et al*. Cardiac Amyloidosis: Evolving Diagnosis and Management: A Scientific Statement From the American Heart Association. *Circulation* 2020;142:e7–22.
11 Leibundgut G, Rohner A, Grize L, *et al*. Dynamic assessment of right ventricular volumes and function by real-time three-dimensional echocardiography: a comparison study with magnetic resonance imaging in 100 adult patients. *J Am Soc Echocardiogr* 2010;23:116–26.
12 Augusto JB, Davies RH, Bhuva AN, *et al*. Diagnosis and risk stratification in hypertrophic cardiomyopathy using machine learning wall thickness measurement: a comparison with human test-retest performance. *Lancet Digit Health* 2021;3:e20–8.
13 Ouyang D, He B, Ghorbani A, *et al*. Video-based AI for beat-to-beat assessment of cardiac function. *Nature New Biol* 2020;580:252–6.
14 Poplin R, Varadarajan AV, Blumer K, *et al*. Prediction of cardiovascular risk factors from retinal fundus photographs via deep learning. *Nat Biomed Eng* 2018;2:158–64.
15 Duffy G, Cheng PP, Yuan N, *et al*. High-Throughput Precision Phenotyping of Left Ventricular Hypertrophy With Cardiovascular Deep Learning. *JAMA Cardiol* 2022;7:386–95.
16 Goto S, Mahara K, Beussink-Nelson L, *et al*. Artificial intelligence-enabled fully automated detection of cardiac amyloidosis using electrocardiograms and echocardiograms. *Nat Commun* 2021;12:2726.
17 Tröbs S-O, Prochaska JH, Schwuchow-Thonke S, *et al*. Association of Global Longitudinal Strain With Clinical Status and Mortality in Patients With Chronic Heart Failure. *JAMA Cardiol* 2021;6:448–56.
18 Oerlemans MIFJ, Rutten KHG, Minnema MC, *et al*. Cardiac amyloidosis: the need for early diagnosis. *Neth Heart J* 2019;27:525–36.
19 Agha AM, Parwani P, Guha A, *et al*. Role of cardiovascular imaging for the diagnosis and prognosis of cardiac amyloidosis. *Open Heart* 2018;5:e000881.
20 Ashish K, Faisaluddin M, Bandyopadhyay D, *et al*. Prognostic value of global longitudinal strain in heart failure subjects: A recent prototype. *Int J Cardiol Heart Vasc* 2019;22:48–9.
21 Dorbala S, Ando Y, Bokhari S, *et al*. ASNC/AHA/ASE/EANM/HFSA/ISA/SCMR/SNMMI Expert Consensus Recommendations for Multimodality Imaging in Cardiac Amyloidosis: Part 1 of 2-Evidence Base and Standardized Methods of Imaging. *Circ Cardiovasc Imaging* 2021;14:e000029.
22 Zhang KW, Vallabhaneni S, Alvarez-Cardona JA, *et al*. Cardiac Amyloidosis for the Primary Care Provider: A Practical Review to Promote Earlier Recognition of Disease. *Am J Med* 2021;134:587–95.
23 Mallus MT, Rizzello V. Treatment of amyloidosis: present and future. *Eur Heart J Suppl* 2023;25:B99–103.